# Optical studies on InP:Fe by Fourier-transform emission and absorption spectroscopy

K. Pressel, K. Thonke,* and A. Dörnen
*IV. Physikalisches Institut, Universität Stuttgart, D-7000 Stuttgart 80, Federal Republic of Germany*

G. Pensl
*Institut für Angewandte Physik, Universtät Erlangen, D-8520 Erlangen, Federal Republic of Germany*
(Received 13 August 1990)

We present highly resolved photoluminescence (PL) and absorption spectra of the internal *d-d*-shell transitions at $Fe^{2+}$ in InP and the related phonon sidebands. By use of the Fourier-transform-infrared technique, the signal-to-noise ratio (SNR) is improved by about two orders of magnitude as compared to conventional dispersive techniques. Thus we are able to resolve new fine structure in the zero-phonon lines of $Fe^{2+}$ in both absorption and PL. This fine structure is identified as shift induced by different iron isotopes. A better SNR also reveals several new features in PL spectra of the phonon sidebands. In absorption measurements $Fe^{2+}$ related spectra in the energetic range of 2800 to 3400 $cm^{-1}$ ($\approx 0.35-0.4$ eV) are recorded, which can be partly attributed to anti-Stokes lines of phonon coupling in emission. Additional peaks at 3103 and 3117 $cm^{-1}$ are interpreted as transitions from the $^5E$ ground state to an excited state of the $^5T_2$ manifold of $Fe^{2+}$.

## I. INTRODUCTION

InP doped with Fe is the standard semi-insulating substrate material in the growth of epitaxial layers for optoelectronic devices. Iron acts as a deep acceptor in InP and thus compensates the unintentional background donor doping. Fe in the 3+ charge state is observed in electron paramagnetic resonance, whereas the existence of the $Fe^{2+}$ state is established by optical measurements. Both photoluminescence (PL) and absorption experiments at low temperatures show a characteristic spectrum of four zero-phonon (ZP) lines, which are attributed to transitions within the $^6D$ ground state of $Fe^{2+}$ ($3d^6$) on the indium site in a tetrahedral crystal field of phoshorus atoms.[1] This paper presents a detailed PL and absorption study of these four ZP lines and their related phonon sidebands.

As compared with conventional grating techniques, Fourier-transform-infrared (FTIR) spectroscopy provides us with an improvement of signal-to-noise ratio (SNR) of two orders of magnitude both for PL and absorption. This becomes evident, e.g., in the observation of a fine structure in the ZP lines of $Fe^{2+}$ in InP as discussed in the following section.

All our measurements are performed on a BOMEM DA3.01 FTIR spectrometer with maximum resolution without apodization of 0.01 $cm^{-1}$ ($\simeq 1.24$ $\mu$eV), which is equipped with an InSb detector. In PL measurements the samples are excited by a krypton-ion laser (647 nm), whereas for absorption measurements the light of a globar lamp is used. The contribution of thermal background radiation, peaking around 1000 $cm^{-1}$, to the emission spectra is eliminated by subtraction of reference spectra recorded without excitation of the samples.

## II. HIGH-RESOLUTION SPECTRA OF THE $Fe^{2+}$ ZERO-PHONON LINES

The energy-level scheme (inset of Fig. 1) shows schematically the splitting of the $^5D$ ground state of $Fe^{2+}$

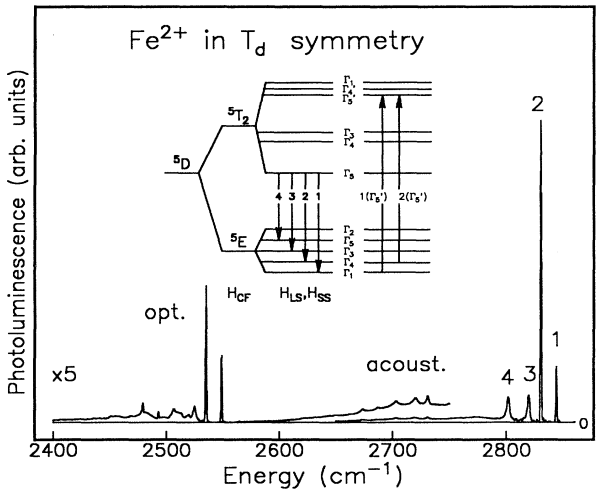


FIG. 1. Level scheme for $Fe^{2+}$ ($3d^6$) in InP, taking into account crystal-field and spin-orbit coupling interactions (inset). The four allowed transitions observed in PL are indicated by arrows with numbers 1–4. Spectrum recorded by FTPL at a resolution of 1 $cm^{-1}$ with an InSb detector (trace). Contributions of thermal background radiation are subtracted. The four sharp zero-phonon transitions at approximately 2850 $cm^{-1}$ are labeled according to the inset. Phonon replicas around 2700 and 2500 $cm^{-1}$ are due to coupling to acoustic- and optic-type modes, respectively.

 

in a tetrahedral environment. A $T_d$ crystal field splits the $^5D$ ground state into two levels $^5E$ and $^5T_2$.[2] Additional spin-orbit (s.o.) ($LS$) coupling splits the $^5E$ and $^5T_2$ states into a manifold of five and six levels, respectively.[2] In optical measurements usually transitions between the lowest $\Gamma_5$ state of the $^5T_2$ manifold and the $\Gamma_1$, $\Gamma_4$, $\Gamma_3$, and $\Gamma_5$ levels of the $^5E$ manifold are observed; the transition $\Gamma_5 \leftrightarrow \Gamma_2$ being forbidden. These allowed transitions are indicated by arrows labeled 1–4 in Fig. 1.

Figure 1 shows the four zero-phonon transitions at $\approx 2800$ cm$^{-1}$ along with the accompanying phonon sideband extending down to 2400 cm$^{-1}$. The coupling to several independent lattice and vibrational modes will be discussed in detail in the following section.

In good agreement with theoretical calculations of Ham and Slack[3] for $Fe^{2+}$ in ZnS, we determined the relative intensities of the four transition lines for $Fe^{2+}$ in InP to be about 4:9:4:3.[4] In our calculations we determined numerically the eigenvalues and eigenstates of the Hamiltonian

$$H = H_{\mathrm{CF}} + H_{\mathrm{s.o.}} = B_4(O_4^0 + 5O_4^4) + \lambda LS \ ,$$

$$L = 2, \quad S = 2, \quad B_4 = Dq/12$$

and fitted the theoretical values to the experimental transition energies; CF denotes crystal field. The eigenvectors are expressed in the basis of eigenstates of the spin and orbital angular momentum operator. In our experiments we observe some deviations from the theoretically derived relative line intensities. Relative line intensities at 4 and 12 K are summarized along with other spectral data of the four ZP lines in Table I. Transition 1 shows the strongest increase in relative line intensity with raising temperature. This fact is ascribed to reabsorption processes.[4]

All four ZP lines show Lorentzian shape at 4 K, but with different half-widths. While in PL measurements the full width at half maximum (FWHM) of lines 1 and 2 is only 0.12 cm$^{-1}$ [Table 1, Fig. 2(a)], the FWHM of lines 3 and 4 is about 2 cm$^{-1}$. Because of the Lorentzian line shape, we believe a nonradiative relaxation process decreases the lifetime of the higher $\Gamma_3(^5E)$ and $\Gamma_5(^5E)$ (Ref. 5) states thus leading to considerable lifetime broadening.

Since the orbital part of the final luminescence states is of character $E$ (or $\Gamma_3$ in the Koster[6] notation), only $E$-type vibrations are effective and cause transitions between $\Gamma_3$ and $\Gamma_1$ or between $\Gamma_5$ and $\Gamma_4$, but not between $\Gamma_4$ and $\Gamma_1$. This results in a lifetime broadening of lines 3 and 4 ending in the $\Gamma_3$ and $\Gamma_5$ states, respectively, but no broadening for lines 1 and 2.

At low sample temperatures, the ZP lines 1 and 2 are very sharp in absorption. Figure 2(a) demonstrates this for line 1, which due to thermalization is the strongest one at a sample temperature of 4 K. We find a FWHM of only 0.016 cm$^{-1}$, close to our resolution limit of 0.01 cm$^{-1}$, and Lorentzian line shape. Taking into account our limited resolution, this means an upper limit for the real linewidth of $(0.016^2 - 0.01^2)^{1/2}$ cm$^{-1}$ $\sim 0.013$ cm$^{-1}$. This electronic transition is the sharpest reported to date in absorption for transition metals in III-V semiconductors. The line shows a fine structure consisting of four components with different amplitude, which is caused by an isotope shift introduced by Fe (see below), and is labeled according to the underlying Fe isotope. The relative intensity of the four fine-structure lines is the same for all samples investigated and independent of sample temperature.

A deconvolution gives an intensity ratio of 5.6:91.5:2.1:0.3, a ratio which is very close to the natural abundance of the four stable iron isotopes $^{54}$Fe (5.8%), $^{56}$Fe (91.8%), $^{57}$Fe (2.1%), and $^{58}$Fe (0.3%). Also the spacing of the components being identical for the ($^{54}$Fe, $^{56}$Fe) and ($^{56}$Fe, $^{58}$Fe) lines with the ($^{57}$Fe) line located halfway between ($^{56}$Fe), ($^{58}$Fe) strongly supports this interpretation.

The identical fine structure can be seen in PL spectra of both lines 1 and 2 [see Fig. 2(b)], although the signal-to-noise ratio is poorer. In addition, in PL the linewidth of both lines is approximately 0.12 cm$^{-1}$, i.e., a factor of $\approx 7$ more than in absorption (recorded on the *same* samples). Since the line shape is still Lorentzian, we again assume a lifetime effect to be responsible for this broaden-

TABLE I. Spectral data of the four dominant zero-phonon lines of $Fe^{2+}$ in InP.

| Line no. | | Final $^5E$ level | Absolute energy (cm$^{-1}$) Abs. (4 K) | Absolute energy (cm$^{-1}$) PL (4 K) | FWHM (cm$^{-1}$) PL 12 K | PL 4 K | absorption 12 K | absorption 4 K | Relative PL line intensity ($^{56}$Fe) 12 K | 3 K | Theor. |
|---|---|---|---|---|---|---|---|---|---|---|---|
| 1 | $^{54}$Fe | $\Gamma_1$ | 2843.54 | 2843.54 | | | | 0.05 | | | |
| | $^{56}$Fe | | 2843.85 | 2843.85 | 3.1 | 0.12 | 0.56 | 0.02 | 44 | 15.6 | 46.7 |
| | $^{57}$Fe | | 2843.99 | | | | | | | | |
| | $^{58}$Fe | | 2844.16 | | | | | | | | |
| 2 | $^{54}$Fe | $\Gamma_4$ | 2829.85 | 2829.86 | | | | | | | |
| | $^{56}$Fe | | 2830.16 | 2830.18 | 2.6 | 0.12 | 0.56 | 0.07 | 100 | 100 | 100 |
| | $^{57}$Fe | | | | | | | | | | |
| | $^{58}$Fe | | | | | | | | | | |
| 3 | | $\Gamma_3$ | | 2819.75 | 3.8 | 1.9 | | | 29.9 | 21.3 | 50.5 |
| 4 | | $\Gamma_5$ | | 2801.79 | 4.4 | 2.2 | | | 28.5 | 24.9 | 34.0 |

ing. This lifetime shortening, taking place only in emission experiments but not in absorption, could have different sources: One possibility is that the lifetime of the $Fe^{2+}$ charge state (in either the $^5T_2$ or $^5E$ constellation) is reduced due to the presence of excess free holes generated by laser excitation, which lead to a charge-transfer reacton $Fe^{2+}+h \rightarrow Fe^{3+}$. Also, nonequilibrium phonons generated during the free-particle or free-exciton capture in the process of excitation of $Fe^{2+}$ could give rise to a lifting of electrons out of the initial state $\Gamma_5$ ($^5T_2$) into one of the higher states of the $^5T_2$ manifold, again reducing the effective lifetime of the initial state.

The correctness of the interpretation of the fine structure as an isotope effect is demonstrated unambiguously by experiments on ion implanted samples. InP nominally free of Fe was implanted at 300 keV with different doses of $^{54}$Fe and annealed at 700 °C for 10 sec with a rapid thermal annealer. PL spectra of line 2 of samples implanted with doses $1\times10^{14}$ cm$^{-2}$ and $3\times10^{14}$ cm$^{-2}$ are compared in Fig. 3 with a spectrum of the annealed starting material. The starting material obviously still contained some unintentional Fe doping. After implantation, the peak ascribed to $^{54}$Fe is increased, reaching for the higher implantation dose an intensity comparable to the $^{56}$Fe peak. In addition to the correct modeling of the optical transitions by the crystal-field model applied to $Fe^{2+}$, this is an independent proof that these transitions occur at a defect containing one optically active Fe atom.

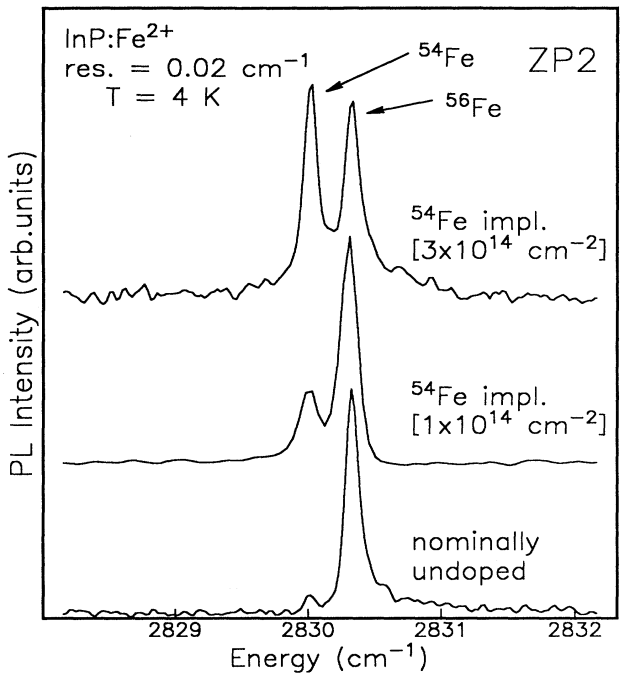


FIG. 3. PL spectrum of zero-phonon line 2 recorded with a resolution of 0.02 cm$^{-1}$. Lower trace: spectrum of nominally undoped, only annealed sample. Upper traces: After implantation of $^{54}$Fe and subsequent annealing, the fine-structure line ascribed to the isotope 54 increases with higher implantation dose.

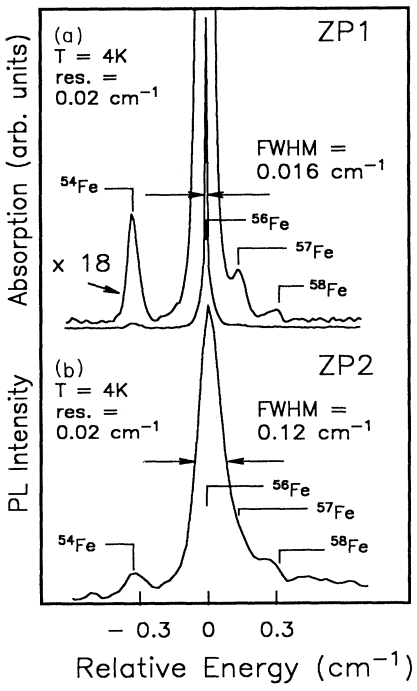


FIG. 2. (a) Absorption spectrum of line 1 recorded at a sample temperature of 4 K with a resolution of 0.02 cm$^{-1}$ (no apodization); the narrow trace of the $^{56}$Fe component recorded with a resolution of 0.01 cm$^{-1}$. The fourfold fine structure is induced by an isotope effect of four stable Fe isotopes $^{54}$Fe, $^{56}$Fe, $^{57}$Fe, and $^{58}$Fe. (b) ZP line 2 in luminescence, recorded with a resolution of 0.02 cm$^{-1}$. The sample temperature is 4 K. The fine structure is identical to that observed in absorption on line 1, although the signal-to-noise ratio is worse.

Before implantation and annealing of the substrate the $Fe^{2+}$ related emissions are not observable. Only after annealing these emissions show up in the unimplanted sample. We obtain a maximal Fe related signal by the annealing of samples at approximately 700 °C. At this temperature probably most of the iron in nominally undoped samples diffuses to the surface. Therefore, more signals are expected in PL measurements, where the sample is excited essentially within the first micrometer.

## III. PHONON SIDEBANDS

### A. Phonon sidebands in photoluminescence

Due to the improved signal-to-noise ratio of FTPL, we could study the phonon sidebands associated with the $Fe^{2+}$ optical transition in more detail than published hitherto.

There are two prominent regions in the phonon sideband (see Fig. 1), which by their energetic spacing can be ascribed to coupling to acoustic-type phonons

(2700 $cm^{-1}$ region) or optic-type phonons (2500 $cm^{-1}$ region), respectively. The rough features were reported already elsewhere.[7,8] By integrating over the total area under the ZP lines and the area under the phonon sideband in a high-resolution emission spectrum we determined a Huang Rhys factor of 0.63, i.e., the coupling to phonons is relatively weak in total.

Within the transverse-acoustical (TA) region, we find coupling of the four ZP lines to several different modes [Fig. 4(a), Table II]: the broad peak at $\approx$2770 $cm^{-1}$ consists of two maxima at about 56 and 69 $cm^{-1}$ below ZP line 2, the most intense ZP line in PL. Since these numbers are very close to the TA($L$) and TA($X$) phonons in InP,[9] and because of the relative broadness of the peaks, we interpret them as coupling to more or less undisturbed lattice modes.

Beside this broad feature, three groups of lines with relative spacings identical to the spacing of the zero-phonon lines, but relative intensities different from those of the ZP lines, show up. In group RM1 (where RM denotes resonant mode), which is displaced by 100 $cm^{-1}$ from the ZP lines, the replica of ZP line 1 is missing. This fact cannot be explained by simple phonon symmetry arguments and is presently not understood. The next two groups RM2 and RM3 are displaced by 157 and 180 $cm^{-1}$, respectively. Since all groups consist of lines with low FWHM (typically 5 $cm^{-1}$), and no conventional lattices modes with these specific energies are known, we ascribe all these groups to coupling of defect-induced resonant modes to the ZP transitions.

In the region around 2500 $cm^{-1}$, corresponding to coupling of optical-type phonons, we observe much more detailed structure than reported before.[7,8] A first sequence of lines, connected by the rake labeled GM1 (where GM1 denotes gap mode) in Fig. 4(b), is displaced from their corresponding ZP lines by 295 $cm^{-1}$. The intensity ratio and half-width of individual components is similar to the ZP lines, although the replica of line 1 is higher here: the ratio 1:2 of ZP lines is 15:100, whereas it is about 1:2 in the replicas. Under high resolution, the pattern induced by the Fe isotope effect is found in the 295 $cm^{-1}$ replicas of 1 and 2 again. Although the phonon energy is close to that of the transverse-optical (TO) phonon in InP [$\nu_{TO}(\Gamma)=308$ $cm^{-1}$ at 4 K, Ref. 10], we ascribe these replicas to a defect-induced gap mode (GM1) instead of lattice TO modes because of the extremely narrow half-width of less than 0.2 $cm^{-1}$ of the two upper lines out of rake GM1. This conflicts with the earlier assignment of Leyral *et al.*,[8] which was based on less clearly resolved spectra.

The next sequence of lines, labeled LM1 (where LM denotes local mode) in Fig. 4(b), originates from coupling to a vibrational mode with energy of 350 $cm^{-1}$. Again, this energy is close to the LO phonon in InP [$\nu_{LO}(\Gamma)=346$ $cm^{-1}$ at 300 K, Ref. 11], but for the similarly small FWHM we attribute these replicas to a local mode LM1.

Besides the two complete sets of replicas, several weak and broad intermediate phonon peaks are observed. Most of them can be interpreted as replicas of the strongest ZP line 2 in PL mediated by coupling of the electronic transition to lattice modes or combination vibrations. A peak at 2521 $cm^{-1}$ is displaced from line 2 by 309 $cm^{-1}$ and is, therefore, ascribed to a resonance of the TO($\Gamma$) lattice mode as observed by Raman spectroscopy at 4 K (308.2 $cm^{-1}$, Ref. 10). Similarly, we ascribe the peak

TABLE II. Spectral data for phonon resonances of ZP lines 1, . . . , 4 in photoluminescence [Figs. 4(a) and 4(b)] and absorption (Fig. 5). For interpretation see text. The energies of the defect specific resonant modes RM1,...,RM3 and gap mode GM1 are slightly different for the defect in the electronic ground state $^5E$ or excited state $^5T_2$; labels with an asterisk denote phonons generated in the $^5T_2$ state. Transitions marked with two asterisks are electronic in nature (see the text).

| Photoluminescence | | Absorption | |
|---|---|---|---|
| relative energy ($cm^{-1}$) | interpretation | relative energy ($cm^{-1}$) | interpretation |
| 56 | TA($L$) | 57 | TA($L$) |
| 69 | TA($X$) | 72 | TA($X$) |
| 100 | RM1 | 103 | RM1* |
| 157 | RM2 | 155 | RM2* |
| 180 | RM3 | | |
| | | (273) | ZP lines** |
| | | (3117 $cm^{-1}$) (abs.) | $\Gamma_1(^5E)\rightarrow\Gamma_5'(^5T_2)$ |
| | | (3103 $cm^{-1}$) (abs.) | $\Gamma_4(^5E)\rightarrow\Gamma_5'(^5T_2)$ |
| 295 | GM1 | 292 | GM1* |
| 309 | TO($\Gamma$) | 307 | TO($\Gamma$) |
| 318 | TO($L$) | | |
| $\approx$342 | GM1+TA($L$) | | |
| 350 | LM1 | | |
| $\approx$372 | TO($L$)+TA($L$) | | |
| 2×295 | 2×GM1 | 2×292 | 2×GM1* |

with 318 $cm^{-1}$ distance to a TO($L$) resonance.

A combination of gap mode GM1 with an acoustical phonon TA($X$), TA($L$) is believed to give rise to a peak at 2482 $cm^{-1}$, whereas the broad feature at 2458 $cm^{-1}$ could come from generation of a combined TO($L$)+TA($L$) vibration.

The relatively intense GM1 replicas are repeated at the double distance to the ZP lines [see inset in Fig. 4(b)], along with a combination with local mode LM1.

Table II lists the spectroscopic data on phonon replicas mentioned in this section. Since detailed theoretical calculation on normal vibrations of Fe and its surrounding in InP are presently not available, a definite assignment of the replicas detected here has to await theoretical work.

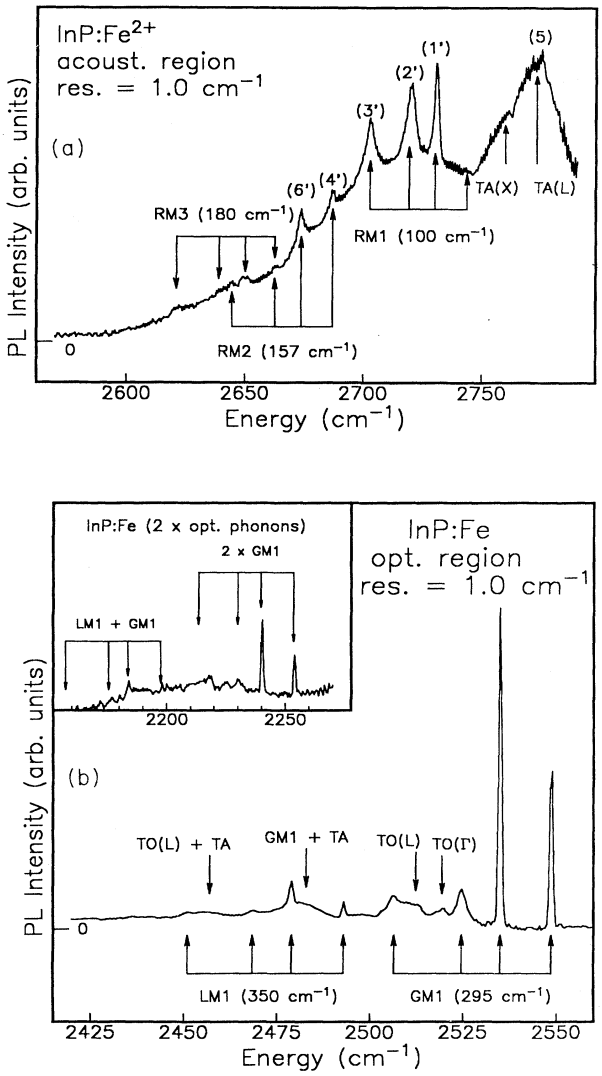


FIG. 4. (a) Phonon sideband in the TA region. In addition to the coupling to undisturbed TA($L$) and TA($X$) lattice modes, we observe sharper replicas of the 4 ZP lines due to three different resonant modes of 100 $cm^{-1}$ (RM1), 157 $cm^{-1}$ (RM2), and 180 $cm^{-1}$ (RM3) energy. Rakes of arrows connect these groups of lines, which have the identical relative energetic spacing as the zero-phonon lines. Note that for mode RM1 the replica of ZP line 1 is missing. Numbers in parentheses reproduce the labeling of Leyral *et al.* (Refs. 7 and 8). (b) FTPL spectrum of phonon replicas in the optical-phonon region. We observe two series of lines introduced by coupling to a defect related gap mode (GM1) of 295 $cm^{-1}$ energy and a localized mode (LM1) with 350 $cm^{-1}$ energy. Weaker peaks in between are interpreted as replicas due to lattice modes or combination vibrations (see text, and Table II). The inset shows a part of the spectrum in the two-phonon region.

### B. Phonon sidebands in absorption

Up to now, only the ZP lines 1–4 were observed in absorption measurements.[1] We report here an "anti-Stokes" phonon sideband, which mirrors to a great part the Stokes phonon sideband found in PL (see Sec. II), but exhibits as well some characteristic differences.

At low temperatures, line 1 dominates the spectrum, since mainly the lowest level $\Gamma_1(^5E)$ is populated; line 2 is weaker (see Fig. 5). Thus mainly the phonon replicas of the strongest line 1 are found in the sideband.

Closest to the ZP lines the double-peaked counterpart of the TA($L$), TA($X$) replica is found; the spacing of the maxima from line 1 again is approximately 56 and 70 $cm^{-1}$, respectively. The two peaks 103 $cm^{-1}$ above the ZP lines 1 and 2 are the counterparts of the resonant mode RM1. The slightly increased vibration energy hints to stronger force constants for this normal mode in the electronically excited $\Gamma_5(^5T_2)$ state as compared with the $^5E$ substates. Both maxima of phonon line RM1 follow in their relative intensity the ratio of ZP lines 1 and 2 on temperature variation. In contrast to the Stokes side,

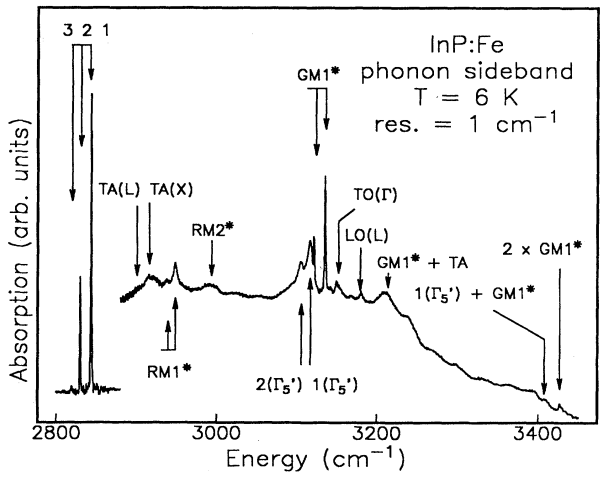


FIG. 5. Phonon sideband related to InP:$Fe^{2+}$ electronic transitions. Most phonons, which couple in emission, are found in absorption again with slightly modified energies and different selection rules. At 3117 $cm^{-1}$ a new transition $1(\Gamma_5')$ is found, which is interpreted as excitation from the lowest $^5E$ substrates into the $\Gamma_5'$ excited state of the $^5T_2$ manifold. The spectrum is partially tampered in the 3000 $cm^{-1}$ region by a broad background absorption band of frozen water vapor.

selection rules seem not to forbid the coupling of this normal mode to line 1. This discrepancy is presently not understood.

Next follows in the spectrum a broader hump about 155 $cm^{-1}$ above ZP line 1, which must be the resonant mode RM2 in the excited electronic state. Similar as in emission, the strongest peaks in the absorption phonon sideband are the resonances of the gap mode GM1*. For this mode, the vibration energy in the $\Gamma_5(^5T_2)$ state is 292 $cm^{-1}$ and thus slightly lower than in the $^5E$ state. Again, both lines follow closely in their relative intensities the ZP lines 1 and 2. The coupling of the local mode LM1 is presumably too weak to be detectable in absorption. Out of the weaker replicas on the Stokes side, only line TO($\Gamma$) in a distance of 306 $cm^{-1}$ to ZP line 1 is resolvable. Beside some weak peaks due to combination modes, the second harmonic of GM1* is observed.

## IV. INTERNAL TRANSITONS AT HIGHER ENERGY IN ABSORPTION

In the absorption spectrum displayed in Fig. 5 two additional peaks labeled $2(\Gamma_5')$ and $1(\Gamma_5')$ show up, which we did not discuss yet. Both components of this resonance just below the gap mode GM1* follow the relative intensities of ZP lines 1 and 2 and have the identical energetic spacing as the latter lines. Therefore, these must be clearly transitions originating in the lowest two sublevels $\Gamma_1$ and $\Gamma_4$ of the $^5E$ orbital state. The half-width of these peaks seems to hint to phonon replicas. But since we could not find corresponding Stokes lines with the identical energetic displacement of 273 $cm^{-1}$ from the ZP lines, we discard this explanation. Instead, we suggest these transitions to be electronic in nature and to end in the excited state $\Gamma_5'$ out of the $^5T_2$ manifold (see inset of Fig. 1).

We consider the increased half-width as a consequence of the reduced lifetime of the final $\Gamma_5'(^5T_2)$ state, due to several possible relaxation channels open for electrons excited into lower lying $^5T_2$ substates. From the half-width of these transitions of $\approx 7$ $cm^{-1}$ a (nonradiative) lifetime of $\approx 0.4$ psec can be estimated, a number in accordance with the assumed thermalization processes.

The assignment pointed out here would mean an energetic splitting between the lowest $^5D$ state $\Gamma_1(^5E)$ and the almost highest state $\Gamma_5'(^5T_2)$ of 3117 $cm^{-1}$ ($\approx 386.5$ meV), the energetic position of this line in the spectrum. We have to compare this number with theoretical calculations based on the crystal-field theory. Using the parameters $Dq = 303.8$ $cm^{-1}$ and $\lambda = -86.6$ $cm^{-1}$ for crystal-field and spin-orbit coupling,[4] an energy of 3272 $cm^{-1}$ is predicted. The deviation of the measured position to lower energies is not unexpected: The excited $^5T_2$ state with its nonvanishing orbital momentum is susceptible to a Jahn-Teller (JT) effect as observed for Fe in ZnS.[3] As a result the $^5T_2$ substates can be drastically lowered in energy (see Figs. 2–4 in Ref. 3). In view of the theoretical predictions for the JT effect, the phonon coupling in the system under investigation is still moderate.

Our interpretation of the 3117 $cm^{-1}$ line is supported by an independent experimental observation: Juhl and co-workers[12] observed by calorimetric absorption spectroscopy several transitions around 0.8 and 1.18 eV, which they interpreted as charge-transfer transitions from the valence band to $Fe^{2+}$ states. We investigated these spectra in more detail and with improved SNR by optical FTIR absorption spectroscopy and could resolve several new features, which will be reported elsewhere.[13] The difference in energy between lines *a* [a transition to the $\Gamma_1(^5E)$ state], and line $\alpha$ of Juhl *et al.* is 3117 $cm^{-1}$ according to our results; i.e., exactly the same energy as that of our resonance $1(\Gamma_5')$ in Fig. 5. We reinterpret lines *a* and *b* of Ref. 12 as excitation of an electron from a shallow, Fe related bound hole state close to the valence-band edge, to the $\Gamma_1(^5E)$ and $\Gamma_4(^5E)$ states, respectively. Line $\alpha$ must be the transition from the same shallow level to the $\Gamma_5'(^5T_2)$ state, instead of a transition from $Fe^{3+}$ to the conduction band producing $Fe^{4+}$ as proposed by Juhl *et al.* Line $\alpha$ has a similar linewidth as our $1(\Gamma_5')$ resonance. For both lines we find in absorption a phonon replica 292 $cm^{-1}$ higher in energy, i.e., the frequency characteristic for the gap mode GM1* in the $^5T_2$ state, demonstrating again for both lines the involvement of the $Fe^{2+}$ $^5T_2$ state. A reassignment of lines *B* and *C* from Ref. 12 will be discussed elsewhere.[13]

## V. SUMMARY

We present highly resolved photoluminescence and absorption spectra of $Fe^{2+}$ in InP, which reveal numerous new features. A fine structure in the zero-phonon lines of the electronic transitions recorded both in absorption and photoluminescence is demonstrated to be induced by an Fe isotope effect. An anti-Stokes phonon sideband, which was not reported hitherto, reveals coupling to different lattice and localized vibrational modes. These absorption results are correlated to highly improved FTPL spectra. From absorptions at 3103 and 3117 $cm^{-1}$ the energetic position of the excited $\Gamma_5'(^5T_2)$ state is derived.

## ACKNOWLEDGMENTS

We thank F. S. Ham for valuable discussions on relaxation processes. The financial support of the Deutsche Forschungsgemeinschaft (DFG), Bonn, Germany, under Contract No. Th-419 is gratefully acknowledged.

*Present address: Abteilung Halbleiterphysik, Universität Ulm, D-7900 Ulm, FRG.

[1]W. H. Koschel, U. Kaufmann, and S. G. Bishop, Solid State Commun. **21**, 1069 (1977).

[2]W. Low and M. Weger, Phys. Rev. **118**, 1119 (1960).

[3]F. S. Ham and G. A. Slack, Phys. Rev. B **4**, 777 (1971).

[4]K. Thonke, K. Pressel, H. U. Hermann, and A. Dörnen, *Proceedings of the 15th International Conference on Defects in Semiconductors, Budapest, 1988,* Vols. 38–41 of the Materials Science Forum (Trans Tech, Aedermannsdorf, Switzerland,

1989), p. 869.

[5]In the following sections we will denote the two orbital states produced by crystal-field splitting with $^5T$ and $^5E$. The states of the fine-structure splitting due to spin-orbit coupling are labeled $\Gamma_1-\Gamma_5$. Thus $\Gamma_3(^5E)$, i.e., describes the $\Gamma_3$ state out of the $^5E$ manifold.

[6]G. F. Koster, J. O. Dimmock, R. G. Wheeler, and H. Statz, *Properties of the 32 Point Groups* (MIT, Cambridge, 1963).

[7]P. Leyral, G. Bremond, A. Nouailhat, and G. Guillot, J. Lumin. **24/25**, 245 (1981).

[8]P. Leyral, C. Charreaux, and G. Guillot, J. Lumin. **40/41**, 329, (1988).

[9]Landolt-Börnstein, *Numerical Data and Functional Relationships in Science and Technology* (Springer-Verlag, Berlin, 1982), Vol. 17a, p. 281ff.

[10]A. Mooradian and G. B. Wright, Solid State Commun. **4**, 431 (1966).

[11]P. H. Borcherds, G. F. Alfrey, D. H. Saunderson, and A. D. B. Woods, J. Phys. C **8**, 2022 (1975).

[12]A. Juhl, A. Hoffmann, D. Bimberg, and H. J. Schulz, Appl. Phys. Lett. **50**, 1292 (1987).

[13]K. Pressel *et al.* (unpublished).